Surface plasmon-mediated photoluminescence boost in graphene-covered $CsPbBr_3$ quantum dots

Guanhua Ying†, Elham Oleiki†, Atanu Jana, Vitaly Osokin, Mutibah Alanazi, Sangeun Cho, Hyunsik Im, Robert A. Taylor*, Youngsin Park*, and Geunsik Lee*

ABSTRACT: The optical properties of graphene (Gr)-covered $CsPbBr_3$ quantum dots (QDs) were studied by micro-photoluminescence (μPL). Compared with bare $CsPbBr_3$ QDs, the PL intensity of the Gr-covered $CsPbBr_3$ QDs is enhanced dramatically, almost by three orders of magnitude. Density functional theory (DFT) calculations were performed to investigate the origin of the PL enhancement by considering different heterojunction models. For the bare $CsPbBr_3$, contacting with Gr on the top side of the $CsPbBr_3$ causes the Dirac point to appear at the center of the $CsPbBr_3$ energy gap. For defective $CsPbBr_3$ with predominantly halide vacancy defects, the surface defect states are passivated when they are covered by Gr. At the same time, the Gr is *n*-doped and corrugated by the defect passivation, whose plasmons possess an energy and momentum in resonance with the photo-generated excitons in the $CsPbBr_3$. Our experimental and theoretical investigations reveal the vital role that a top contact of Gr has in producing dramatic PL enhancement of $CsPbBr_3$ dot emission.

KEYWORDS: perovskite quantum dots, graphene coating, photoluminescence; surface plasmon-induced resonance, defect passivation

INTRODUCTION

All inorganic lead halide perovskites (LHP) $CsPbX_3$ (X = Cl, Br or I)[1] have emerged as a promising material for a wide range of optoelectronic applications such as solar cells,[2–4] light-emitting diodes,[5] and photodetectors[6] due to their higher stability compared to their organic-inorganic counterparts.[7–9] $CsPbBr_3$ has excellent optoelectronic properties, including an extremely high photoluminescence (PL) quantum yield, narrow emission bandwidth, and long carrier diffusion length and lifetime.[10,11] Furthermore, its emission energy can be tuned from 2.29 eV to 2.53 eV by synthesizing it in various structures like bulk single crystals, thin films, nanocrystals (NCs), nanowires, and quantum dots (QDs).[12–14] The origin of the emissions originates from a single exciton, lasing due to biexcitonic emission,[15] cavity lasing from micro/nanowire,[16] triplet excitonic emission,[17] and superfluorescence.[18] Using LHPs in heterojunctions is an effective way to improve their optoelectronic properties. In particular, a graphene (Gr) sheet with ultrahigh carrier mobility[19] and wavelength independent light absorption[20] has been hybridized with $CsPbBr_3$ to improve its optoelectronic performance.[6,21,22,23,24,25,26,27] Namely, enhanced visible light absorption was observed in $CsPbBr_3$ NCs/Gr heterostructures.[21,22] Interfacial energy level alignment of $CsPbBr_3$ NCs/Gr junction facilitated electron transfer from the $CsPbBr_3$ light absorber to the Gr electron transport layer, resulted in strong PL quenching and improved photo response.[6,21] In addition, it is well-known that surface defects can introduce non-radiative trap states in LHPs.[28–30] Thus, the passivation of surface defects

can significantly affect the PL properties. Research has been conducted on a variety of molecules with different functional groups to passivate surface defects in LHPs'.[31] Notably, it was shown that by encapsulating $CsPbBr_3$ NCs with Gr, surface defect states generated by Pb vacancies were passivated, and the photoluminescence quantum yield (PLQY) was enhanced by a factor of seven.[23] Another effective method to improve the quantum efficiency of optoelectronic heterojunctions is PL enhancement by the resonant excitation of surface plasmons.[32–34] In particular, it has been reported that for Gr/semiconductor interfaces, Gr plasmons were resonantly activated by radiative recombination of electron-hole pairs from a semiconductor photo absorber. Consequently, Gr plasmons transformed into propagating photons through interaction with interface corrugations explaining the observed enhancement in PL.[35–38]

Here, we report a dramatic enhancement of the PL intensity of Gr-covered $CsPbBr_3$ QDs compared to bare $CsPbBr_3$ QDs. The origin of the PL enhancement was characterized by employing density functional theory (DFT) to calculate the electronic structure of the $Gr/CsPbBr_3/SiO_2$ heterosystem. The DFT calculation results revealed that the interfacial electrostatic potential barriers at the $Gr/CsPbBr_3$ interface in the $Gr/CsPbBr_3/SiO_2$ heterosystem are high enough to prevent carrier leakage from the perovskite to the Gr layer leading to a high radiative recombination rate. This is in contrast to existing reports about $CsPbBr_3/Gr/SiO_2$ heterosystem whose radiative recombination rate suppressed due to the electron transfer from $CsPbBr_3$ to Gr.

RESULTS AND DISCUSSION

The detailed crystal structure of the $CsPbBr_3$ QDs was investigated using transmission electron microscopy (TEM). Figure 1 shows the TEM images of the $CsPbBr_3$ QDs. The individual QDs tend to aggregate forming clusters of various sizes. Compared to previous reports for well-aligned $CsPbBr_3$ QDs,[39,40,41,42,43,44,45,46] our small QD clusters have a tetragonal shape with dimensions randomly distributed from ~10 to 20 nm, which suggests that the emission energy should show an ensemble effect arising from interacting QDs.

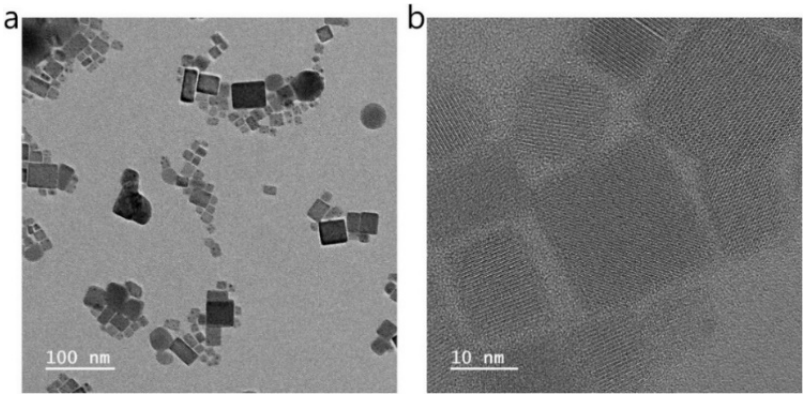

Figure 1. a) Transmission electron microscopy images of $CsPbBr_3$ QD clusters. b) High resolution transmission electron microscopy image of individual dots in a cluster. The QDs were ultra-sonicated for 10 min in toluene solution and then dispersed on the TEM grid.

Figure 2 presents power-dependent PL spectra for bare $CsPbBr_3$ QDs and Gr-covered $CsPbBr_3$ QD clusters measured at 4.2 K. For the bare $CsPbBr_3$ QDs, a single excitonic emission near 2.33 eV with a full width at half maximum (FWHM) of ~1.7 nm (~1.5 meV) is observed at an excitation power of 10 μW. It should be noted that by increasing the excitation power, new blue-shifted emission lines appear. All the power-dependent emission peaks were fitted to extract physical parameters such as integrated intensity, FWHM, and emission energy. The integrated intensity of the specific emission line

(marked red dots, L, in Figure 2a) shows an S shape behavior (Figure S1a), which is indicative of stimulated emission. Unlike the bare $CsPbBr_3$ QDs, the PL spectra of the Gr-covered $CsPbBr_3$ QDs show several emission peaks even at a very low excitation power of 2 nW. In addition, it shows a much brighter emissive response with high signal-to-noise ratio. At this level of pumping strength, no identifiable emission profile can be retrieved for the bare $CsPbBr_3$ QDs. Also, no new emission peaks emerge and none of the original peaks show a blueshift below an excitation power of a few tens of μW. The integrated PL intensity of the Gr-covered $CsPbBr_3$ QDs shows a linear dependence with excitation power (Figure S1b). Although no stimulated emission peak was observed in this case, the PL quantum efficiency was significantly enhanced. On the other hand, the PL intensity of the perovskite/Gr/SiO_2 heterostructure is quenched (Figure S2), consistent with the previous reports.[21,24] The enhanced PL intensity of the Gr-covered $CsPbBr_3$ QDs could originate from the surface defect passivation, surface plasmon resonance effect, and Fermi energy (E_F) band alignment *etc*.

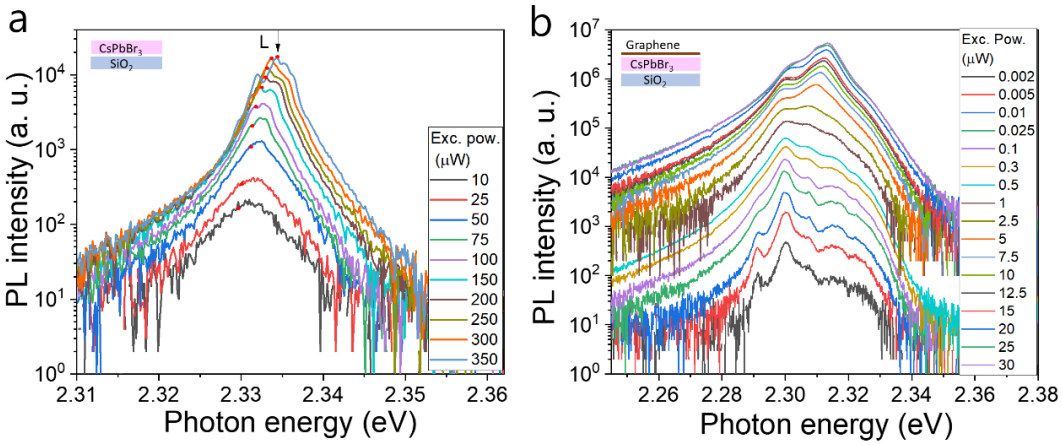

Figure 2. PL comparison between Gr-coated and uncoated $CsPbBr_3$ QD clusters at 4.2 K. a) Power-dependent μPL spectra measured for the bare $CsPbBr_3$ QD cluster. Lasing is observed at high pumping fluence. b) Power-dependent μPL spectra taken for a Gr-coated $CsPbBr_3$ (Gr/$CsPbBr_3$/SiO_2) heterostructure clusters. Two distinguishable emission lines at 2.313 eV and 2.300 eV are present. With increasing pumping strength,

the main emission evolves from the 2.300 eV peak towards the 2.313 eV peak.

To investigate the origin of the PL intensity quenching, we explored the electronic structure of $CsPbBr_3/Gr/SiO_2$ heterostructure by performing the DFT calculations. The model structure is described in the methods section and is illustrated in Figure 3a and Figure S3a. According to the DFT calculation results, the $CsPbBr_3/Gr$ interface is stabilized through weak van der Waals interaction with an interlayer distance of 3.4 Å and binding energy of -0.03 eV per carbon atom (Eq. S1). The ground state electronic band structure of the $CsPbBr_3/Gr/SiO_2$ heterostructure is depicted (Figure 3a), where a perovskite symmetry slab with $PbBr_2$ termination type is employed. The $CsPbBr_3$ layer shows a direct band gap of 1.9 eV located at the Γ point. In addition, upon the formation of the $CsPbBr_3/Gr$ interface, electrons transfer from the $CsPbBr_3$ to the Gr, indicating the *n*-doped character of Gr as evidenced by the Dirac point appearing below the E_F level. Moreover, the Fermi level is strongly pinned to the perovskite's valence band maximum (VBM). Therefore, under the illumination of the perovskite light absorber, electrons will readily transfer from the Gr layer to photo-generated empty states in the perovskite valance band. Consequently, the radiative recombination of photo-excited electron-hole pairs in perovskite will be suppressed, leading to PL quenching in $CsPbBr_3/Gr/SiO_2$ system, which is in agreement with previous reports[21,24,25]. The Fermi level pinning at the perovksite VBM is confirmed to appear when the $PbBr_2$-terminated surface is in contact with Gr/SiO_2, being independent of the terminal type of the opposite side (Figure S5b).

We also modeled the $Gr/CsPbBr_3/SiO_2$ heterostructure (Figure 3b and Figure S3b) to

determine the reason for the PL intensity enhancement. Like the $CsPbBr_3/Gr/SiO_2$ heterostructure, the interfacial interaction at the $Gr/CsPbBr_3$ junction is of van der Waals type with an interlayer distance of 3.3 Å and a binding energy of -0.03 eV per carbon atom (Eq. S2). The ground state electronic band structure of the $Gr/CsPbBr_3/SiO_2$ heterostructure is shown in Figure 3b. The $CsPbBr_3$ layer exhibits a direct band gap of 1.80 eV at the Γ point, which is slightly reduced compared with $CsPbBr_3/Gr/SiO_3$ heterostructure, and Gr's Dirac cone is located between the Γ and X points. Interacting with the SiO_2 interface dipole increases the $CsPbBr_3$ work function, leading to a downward shift of its VBM and CBM. This, in turn, enhances the interfacial electrostatic potential barrier for charge transfer at the graphene/$CsPbBr_3$ interface which is evident by comparing the position of the perovskite's VBM and CBM relative to the graphene Dirac point (Figure 3b). Furthermore, following the downshift of the perovskite energy levels, the interfacial orbital coupling at the $Gr/CsPbBr_3$ interface is suppressed. Therefore, the formation of the $Gr/CsPbBr_3/SiO_2$ heterostructure does not result in charge transfer at the Gr/perovskite interface in its ground state, even for the other termination types of the perovskite layer (Figure S4d-f). Under illumination, the interfacial potential barriers are high enough to prevent carrier leakage from the perovskite layer resulting in the enhancement of radiative recombination compared to $CsPbBr_3/Gr/SiO_2$ heterostructure. Another possibility for explaining the PL enhancement could be associated with a surface stabilization effect *via* passivation. However, as we have shown in our previous work on passivation effects,[23] although Gr can potentially mediate the surface tension to some extent due to the structural

similarity between $CsPbBr_3$ and $MAPbBr_3$, it is not able to provide stable bonding (as $Pb(OH)_2$),[47] or as in the case of $MAPbBr_3$ covered with Gr.[23] The relatively smaller size of the Cs^+ cation results in a less stable tetragonal or orthorhombic unit cell configuration; hence, the use of Gr cannot optimize the geometry.

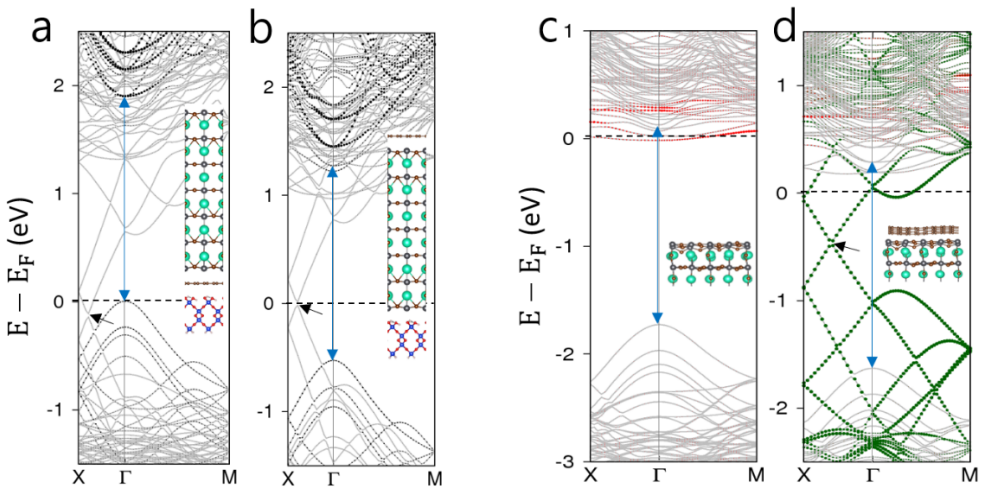

Figure 3. Calculated band structure of (a) $CsPbBr_3/Gr/SiO_2$ (inset: side view along [100] of the model heterostructure) (b) $Gr/CsPbBr_3/SiO_2$. For easier recognition of the $CsPbBr_3$ band edges, the Pb bulk atom's 6p orbital contribution is shown by black circles. (c) $CsPbBr_3$ with a V_{Br} surface defect (inset: side view along [100] of the top 4 atomic layers of the model structure). (d) a defected $CsPbBr_3/Gr$ interface (inset: side view along the [100] interface model structure with a perovskite top 4 atomic layers). Red circles show the contribution of the under-coordinated Pb atom below the V_{Br} site, and the carbon p_z orbital contribution is indicated by green circles. In all band structures, the electronic transition between the $CsPbBr_3$ band edges is indicated by the blue arrow. Gr's Dirac point is indicated by the black arrow in (a), (b), and (d). Atomic color scheme: Cs (green), Pb (gray), Br (brown), Si (blue), O (red), H (pink), C (brown).

The passivation of surface defects can significantly affect the PL properties of MHP nanostructures. Many researchers have investigated using a variety of molecules with

different functional groups to passivate the MHPs' surface defects[31]. In addition, it was shown that by encapsulating MHP NCs with Gr, surface defect states generated by Pb vacancies were passivated, and the PLQY was enhanced seven times[23]. Motivated by these findings, we explored the structural and electronic properties of a defected $CsPbBr_3$ layer with and without Gr on its surface. Since a Br vacancy (V_{Br}) is reported to be the predominant defect in $CsPbBr_3$ perovskites,[48,49] we introduced a V_{Br} into a $PbBr_2$-terminated $CsPbBr_3$ (001) surface. The optimized geometry for the defected interface (Figure 3d inset) indicates a structural distortion in the perovskite top layers caused by V_{Br}.

The Gr is physisorbed on the perovskite surface with a binding energy of -0.03 eV per carbon atom (Eq. S3). We should note that the Gr deformation is an artifact of our model supercell. As shown in Figure 3c, the V_{Br} generates a localized trap state close to the $CsPbBr_3$ conduction band minimum (CBM) which can act as a center for non-radiative recombination and suppress the PL intensity. This is another possibility which might explain PL quenching in $CsPbBr_3$/Gr/SiO_2 heterostructures. However, after covering defected $CsPbBr_3$ with Gr, carbon p_z states hybridized with Pb dangling bond states and shifted them upward to the perovskite conduction band (Figure 3d). Therefore, the Gr adsorption on the defected $CsPbBr_3$ surface eliminates non-radiative recombination centers leading to PL enhancement in the Gr/$CsPbBr_3$/SiO_2 system. It should be noted that upon passivation of the V_{Br} defect, the Gr is *n*-doped (Figure 3d) with a charge density of 10^{13} cm^{-2} (Eq. S4).[50] Similar results are obtained for the Gr/$CsPbBr_3$ interface consisting of the perovskite with a CsBr termination (Figure S6).

Enhanced PL emission due to a resonant surface plasmon-exciton coupling effect has been reported.[44,51,52,37,53] Considering the semi-metallic nature of Gr, the large PL enhancement of the Gr/$CsPbBr_3$/SiO_2 heterosystem could be understood in terms of the resonant excitation of graphene plasmon modes[37,35,36,54]. The perovskite's photogenerated excitons can induce resonant plasmon modes in the Gr layer. However, because of the considerable momentum mismatch between Gr's plasmons and photons in free space, a lateral modulation periodicity on the Gr[35,36] or its substrate[37] is required to resolve the momentum mismatch and transform the excited plasmon mode to the light emission. The dispersion relation of the Gr plasmon in the random phase approximation is

$$\omega(q) = \left[\frac{n_e\, e^2}{\epsilon_0\,(1+\epsilon_b)m^*}\,|q| + \frac{3}{4}\,v_F^2\,q^2\right]^{1/2}$$

where q is in-plane wave number, n_e is the electron density, ϵ_0 is the vacuum permittivity, ϵ_b is the substrate static dielectric constant, m^* is electron effective mass in Gr and v_F is its Fermi velocity.[37,55,56] We supposed that the Gr plasmon could be resonantly excited at perovskite band gap energy of 2.3 eV and calculated the in-plane momentum q from our calculated $n_e = 10^{13}$ cm^{-2}, using $\epsilon_b = 18.6$ for the $CsPbBr_3$ substrate,[28,57] $m^* = 0.077$ m_e,[37] where m_e is the free electron mass, and $v_F = 1.12 \times 10^6$ m/s.[37] We obtained $q = 2\pi/1.8$ nm^{-1}, indicating a lateral modulation periodicity of $a = 1.8$ nm at the Gr/$CsPbBr_3$ interface would be required to extract light from the Gr's plasmon. Due to the presence of V_{Br} defects, the surface structure of $CsPbBr_3$ is distorted and not perfectly flat, resulting in interface corrugations on the order of a few nm. While it may not be feasible to measure a=1.8 nm experimentally, this value is consistent with the lateral distance of

1.68 nm between V_{Br} surface defects in our model structure Thus, the resonant activation of a Gr plasmon at the perovskite band gap, and its conversion to photons *via* interaction with interface surface corrugations, explains the observed PL enhancement for the Gr/$CsPbBr_3$/SiO_2. We also conducted TRPL measurements on bare and Gr-covered CsPbBr3 NCs. Results show a faster decay component for the Gr-covered $CsPbBr_3$ NCs compared to the bare ones (Figure S7). This is consistent with the faster decay channels enabled by a surface plasmon-polariton interaction.[58] Also, the presence of a Gr layer creates an asymmetric Fabry Perot cavity for optical confinement between the Gr layer and the surface of the NCs, thus boosting the excitation efficiency.

Figure 4a demonstrates a TRPL comparison of the 2.313 eV peak from Figure 2b at pumping strengths of 0.2 μW and 22 μW, respectively. A shortened lifetime is observed at higher pumping fluence. The potential causes for such a fast component can originate either from an Auger process or a coupling effect through modification of the density of the effective photon states. It is unlikely that an Auger process could have such a significant impact at this low level of excitation fluence. Further evidence is provided by the fact that the short lifetime component disappears at higher temperatures (Figure 4b) supporting the argument that the peak arises from coupled emission. It is expected that the coupling effect will be reduced as the temperature rises.[59] Increasing temperature can introduce randomness and hence introduce distortion to the dipole alignment and coherence. The Auger effect shouldn't disappear quickly with increasing temperature and the disorder introduced through the increased entropy weakens the coherent interaction among the QDs, which would quickly reduce the optical resonance

as observed from the diminishing fast component below 100 K. The Gr-coating together with the microscopic dipole alignment significantly boost the PL efficiency of the system as whole. Note that the microscopic oscillating dipoles align with each other leading to the formation of a macroscopic dipole within a dephasing time limit. The resulting emission will have both enhanced coherence and directionality. Like other semiconductor QDs, the size and geometry of a matrix of $CsPbBr_3$ QDs are subject to variations. Although the spin coating process has helped to spatially filter the QD clusters based on their sizes, we often found that clusters of similar dimensions are clumped together. It is therefore possible to excite multiple QD arrays under slightly different conditions within a single laser spot. In most cases, the QD clusters produce independent signals given their distinct emission centers. However, clusters of very similar geometric character, or even two closely alike matrices of QDs within a single cluster, can sit in close proximity such that their individual collective behaviors can overlap and they can interact with each other.

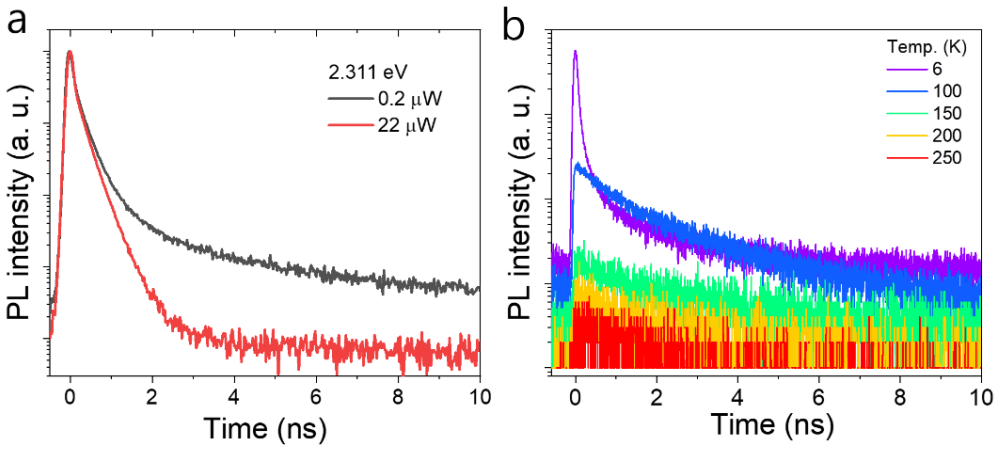

Figure 5. Time-resolved PL of a coupled QD system as in Figure 2b. a) Comparison of the time-resolved PL response at very low excitation fluence (0.2 μW) and relatively high pumping fluence (22 μW) from the 2.313 eV at 4.2 K. b) Time-resolved PL series

taken under different temperatures from the coupled emission site.

CONCLUSIONS

In summary, we have demonstrated the optical characterization of the bare $CsPbBr_3$ QDs and graphene-covered $CsPbBr_3$ QDs by micro-photoluminescence and density functional theory calculations. Compared with bare $CsPbBr_3$ QDs, the PL intensity of the Gr-covered $CsPbBr_3$ QDs is enhanced dramatically, almost by three orders of magnitude. The DFT calculation results showed that contacting Gr on the top side of $CsPbBr_3$ causes the Dirac point to appear at center of $CsPbBr_3$ energy gap, in contrast to the Fermi level pinning behavior to the valence band edge reported for bottom side contact as in $CsPbBr_3/Gr/SiO_2$. Thus, carrier leakage is prevented for the Gr covered $CsPbBr_3$ with a high radiative recombination rate. In addition, the perovskite's surface defects are passivated *via* graphene covering, suppressing the non-radiative recombination of photo-generated charge carriers compared to uncovered perovskite QDs. Furthermore, resonant excitation of graphene plasmons by the perovskite's photogenerated excitons, followed by conversion to photons thorough interaction with graphene/$CsPbBr_3$ interface corrugations, substantially enhances the photoemission from graphene/$CsPbBr_3/SiO_2$ heterosystem. Our experimental and theoretical investigations reveal a vital role of top side contact of graphene for dramatic PL enhancement of $CsPbBr_3$. The graphene covered $CsPbBr_3$ QD clusters can significantly improve the PL efficiency through a surface plasmon polariton effect.

ASSOCIATED CONTENT

Data Availability Statement

The data that support the findings of this study are available from the corresponding author upon reasonable request.

*Supporting Information

The Supporting Information is available free of charge at https://pubs.acs.org/doi/0000000.

AUTHOR INFORMATION

Corresponding Authors

Robert A. Tayler - *Clarendon Laboratory, Department of Physics, University of Oxford, Parks Road, Oxford OX1 3PU, UK*; orcid.org/0000-0003-2578-9645; Email: robert.taylor@physics.ox.ac.uk

Youngsin Park - *Department of Chemistry, College of Natural Science, Ulsan National Institute of Science and Technology, Ulsan 44919, Korea; Clarendon Laboratory, Department of Physics, University of Oxford, Parks Road, Oxford OX1 3PU, UK* orcid.org/0000-0002-1789-750X; Email: ysinpark@unist.ac.kr

Geunsik Lee - *Department of Chemistry, College of Natural Science, Ulsan National Institute of Science and Technology, Ulsan 44919, Korea*; orcid.org/0000-0002-2477-9990; Email: gslee@unist.ac.kr

Authors

Guanhua Ying - *Clarendon Laboratory, Department of Physics, University of Oxford, Parks Road, Oxford OX1 3PU, UK*

Elham Oleiki - *Department of Chemistry, College of Natural Science, Ulsan National Institute of Science and Technology, Ulsan 44919, Korea*

Atanu Jana - *Division of Physics and Semiconductor, Dongguk University, Seoul 04620, Korea;* orcid.org/ 0000-0001-6566-0438

Vitaly Osokin - *Clarendon Laboratory, Department of Physics, University of Oxford, Parks Road, Oxford OX1 3PU, UK*

Mutibah Alanazi - *Clarendon Laboratory, Department of Physics, University of Oxford, Parks Road, Oxford OX1 3PU, UK*

Sangeun Cho - *Division of Physics and Semiconductor, Dongguk University, Seoul 04620, Korea*

Hyunsik Im - *Division of Physics and Semiconductor, Dongguk University, Seoul 04620, Korea*

Complete contact information is available at:

https://pubs.acs.org/000000

Author Contributions

G.Y and E.O contributed equally to this work.

Notes

The authors declare no competing financial interest.

ACKNOWLEDGMENTS

This work was supported from the National Research Foundation of Korea (NRF) grant funded by the Korea government (MSIT) (2021R1A2C1006113 and 2021R1A2C1006039). This work was supported by the National Supercomputing Center with supercomputing resources, including technical support (No. KSC-2022-CRE-0497).

REFERENCES

(1) Wooster, W. A.; M, C. K. Crystal Structure and Photoconductivity of Caesium Plumbohalides Nuclear Magnetic Resonance in ~-Brass. *Proc. Arner. Acad* **1936**, *93* (1955), 131.

(2) Liu, M.; Johnston, M. B.; Snaith, H. J. Efficient Planar Heterojunction

Perovskite Solar Cells by Vapour Deposition. *Nature* **2013**, *501* (7467), 395–398. https://doi.org/10.1038/nature12509.

(3) Green, M. A.; Ho-Baillie, A.; Snaith, H. J. The Emergence of Perovskite Solar Cells. *Nature Photonics* **2014**, *8* (7), 506–514. https://doi.org/10.1038/nphoton.2014.134.

(4) Podolsky, B.; Rosen, N.; Clauser, J. F.; Steinberg, A. M.; Chiao, R. Y.; Vaziri, A.; Weihs, G.; Zeilinger, A.; Bennink, R. S.; Bentley, S. J.; Boyd, R. W.; Ratschbacher, L.; Fedrizzi, A.; Langford, N. K.; Zeilinger, A.; Beijersbergen, M. W.; Spreeuw, R. J. C.; Woerdman, J. P.; Weihs, G.; Zeilinger, A.; Leach, L.; Buller, G. S.; Padgett, M. J.; Andersson, E.; Miatto, F.; Eliel, E. R.; Woerdman, J. P.; Meystre, P.; Schwab, K.; Agarwal, G. S.; Boyd, R. W.; Giovannini, D.; Barnett, S. M.; Padgett, M. J.; Florijn, H. C. B.; Exter, M. P. Van; Pykacz, J.; Nomoto, S. M.; Schubert, W. H.; Novenstern, M. D.; Davis, J. A.; Bandres, M. A.; Broky, J.; Dogariu, A.; Christodoulides, D. N.; Fiorentino, M.; Wong, F. N. C.; Herbst, T.; Poppe, A.; Jennewein, T.; Zeilinger, A.; Hage, B.; Buchler, B.; Lam, P. K.; Maurer, C.; Bernet, S. References and Notes 1. **2012**, *338* (November), 643–648.

(5) Cho, H.; Jeong, S. H.; Park, M. H.; Kim, Y. H.; Wolf, C.; Lee, C. L.; Heo, J. H.; Sadhanala, A.; Myoung, N. S.; Yoo, S.; Im, S. H.; Friend, R. H.; Lee, T. W. Overcoming the Electroluminescence Efficiency Limitations of Perovskite Light-Emitting Diodes. *Science* **2015**, *350* (6265), 1222–1225. https://doi.org/10.1126/science.aad1818.

(6) Kwak, D. H.; Lim, D. H.; Ra, H. S.; Ramasamy, P.; Lee, J. S. High Performance Hybrid Graphene-CsPbBr3-: XIx Perovskite Nanocrystal Photodetector. *RSC Advances* **2016**, *6* (69), 65252–65256. https://doi.org/10.1039/c6ra08699c.

(7) Liang, J.; Wang, C.; Wang, Y.; Xu, Z.; Lu, Z.; Ma, Y.; Zhu, H.; Hu, Y.; Xiao, C.; Yi, X.; Zhu, G.; Lv, H.; Ma, L.; Chen, T.; Tie, Z.; Jin, Z.; Liu, J. All-Inorganic Perovskite Solar Cells. *Journal of the American Chemical Society* **2016**, *138* (49), 15829–15832. https://doi.org/10.1021/jacs.6b10227.

(8) Kulbak, M.; Gupta, S.; Kedem, N.; Levine, I.; Bendikov, T.; Hodes, G.; Cahen, D. Cesium Enhances Long-Term Stability of Lead Bromide Perovskite-Based Solar Cells. *Journal of Physical Chemistry Letters* **2016**, *7* (1), 167–172. https://doi.org/10.1021/acs.jpclett.5b02597.

(9) Wang, P.; Zhang, X.; Zhou, Y.; Jiang, Q.; Ye, Q.; Chu, Z.; Li, X.; Yang, X.; Yin, Z.; You, J. Solvent-Controlled Growth of Inorganic Perovskite Films in Dry Environment for Efficient and Stable Solar Cells. *Nature Communications* **2018**, *9* (1), 1–7. https://doi.org/10.1038/s41467-018-04636-4.

(10) Swarnkar, A.; Chulliyil, R.; Ravi, V. K.; Irfanullah, M.; Chowdhury, A.; Nag, A. Colloidal CsPbBr3 Perovskite Nanocrystals: Luminescence beyond Traditional Quantum Dots. *Angewandte Chemie - International Edition* **2015**, *54* (51), 15424–15428. https://doi.org/10.1002/anie.201508276.

(11) Kang, J.; Wang, L. W. High Defect Tolerance in Lead Halide Perovskite CsPbBr3. *Journal of Physical Chemistry Letters* **2017**, *8* (2), 489–493.

https://doi.org/10.1021/acs.jpclett.6b02800.

(12) Rainoì, G.; Nedelcu, G.; Protesescu, L.; Bodnarchuk, M. I.; Kovalenko, M. V.; Mahrt, R. F.; Stöferle, T. Single Cesium Lead Halide Perovskite Nanocrystals at Low Temperature: Fast Single-Photon Emission, Reduced Blinking, and Exciton Fine Structure. *ACS Nano* **2016**, *10* (2), 2485–2490. https://doi.org/10.1021/acsnano.5b07328.

(13) Stoumpos, C. C.; Malliakas, C. D.; Peters, J. A.; Liu, Z.; Sebastian, M.; Im, J.; Chasapis, T. C.; Wibowo, A. C.; Chung, D. Y.; Freeman, A. J.; Wessels, B. W.; Kanatzidis, M. G. Crystal Growth of the Perovskite Semiconductor CsPbBr3: A New Material for High-Energy Radiation Detection. *Crystal Growth and Design* **2013**, *13* (7), 2722–2727. https://doi.org/10.1021/cg400645t.

(14) Ying, G.; Jana, A.; Osokin, V.; Farrow, T.; Taylor, R. A.; Park, Y. Highly Efficient Photoluminescence and Lasing from Hydroxide Coated Fully Inorganic Perovskite Micro/Nano-Rods. *Advanced Optical Materials* **2020**, *8* (23). https://doi.org/10.1002/adom.202001235.

(15) Yakunin, S.; Protesescu, L.; Krieg, F.; Bodnarchuk, M. I.; Nedelcu, G.; Humer, M.; De Luca, G.; Fiebig, M.; Heiss, W.; Kovalenko, M. V. Low-Threshold Amplified Spontaneous Emission and Lasing from Colloidal Nanocrystals of Caesium Lead Halide Perovskites. *Nature Communications* **2015**, *6*, 8056. https://doi.org/10.1038/ncomms9056.

(16) Wenna Du, Shuai Zhang, Jia Shi, Jie Chen, Zhiyong Wu, Yang Mi, Zhixiong

Liu, Yuanzheng Li, Xinyu Sui, Rui Wang, Xiaohui Qiu, Tom Wu, Yunfeng Xiao, Qing Zhang, X. L. Strong Exciton−Photon Coupling and Lasing Behavior in All- Inorganic CsPbBr3 Micro/Nanowire Fabry-Pérot Cavity. *ACS Photonics* **2018**, *5*, 2051–2059.

(17) Becker, M. A.; Vaxenburg, R.; Nedelcu, G.; Sercel, P. C.; Shabaev, A.; Mehl, M. J.; Michopoulos, J. G.; Lambrakos, S. G.; Bernstein, N.; Lyons, J. L.; Stöferle, T.; Mahrt, R. F.; Kovalenko, M. V.; Norris, D. J.; Rainò, G.; Efros, A. L. Bright Triplet Excitons in Caesium Lead Halide Perovskites. *Nature* **2018**, *553* (7687), 189–193. https://doi.org/10.1038/nature25147.

(18) Rainò, G.; Becker, M. A.; Bodnarchuk, M. I.; Mahrt, R. F.; Kovalenko, M. V.; Stöferle, T. Superfluorescence from Lead Halide Perovskite Quantum Dot Superlattices. *Nature* **2018**, *563* (7733), 671–675. https://doi.org/10.1038/s41586-018-0683-0.

(19) A. K. Geim, K. S. N. The Rise of Graphene. *Narture Materials* **2007**, *6*, 183–191. https://doi.org/10.1038/nmat1849.

(20) Nair, R. R.; Blake, P.; Grigorenko, A. N.; Novoselov, K. S.; Booth, T. J.; Stauber, T.; Peres, N. M. R.; Geim, A. K. Fine Structure Constant Defines Visual Transparency of Graphene. *Science* **2008**, *320* (5881), 1308. https://doi.org/10.1126/science.1156965.

(21) Yun, J.; Fan, H.; Zhang, Y.; Huang, R.; Ren, Y.; Guo, M.; An, H.; Kang, P.; Guo, H. Enhanced Optical Absorption and Interfacial Carrier Separation of CsPbBr3/Graphene Heterostructure: Experimental and Theoretical Insights.

ACS Applied Materials and Interfaces **2020**, *12* (2), 3086–3095. https://doi.org/10.1021/acsami.9b13179.

(22) Lee, Y.; Kwon, J.; Hwang, E.; Ra, C. H.; Yoo, W. J.; Ahn, J. H.; Park, J. H.; Cho, J. H. High-Performance Perovskite-Graphene Hybrid Photodetector. *Advanced Materials* **2015**, *27* (1), 41–46. https://doi.org/10.1002/adma.201402271.

(23) Park, Y.; Jana, A.; Myung, C. W.; Yoon, T.; Lee, G.; Kocher, C. C.; Ying, G.; Osokin, V.; Taylor, R. A.; Kim, K. S. Enhanced Photoluminescence Quantum Yield of MAPbBr3 Nanocrystals by Passivation Using Graphene. *Nano Research* **2020**, *13* (4), 932–938. https://doi.org/10.1007/s12274-020-2718-8.

(24) Youngbin Lee , Jeong Kwon , Euyheon Hwang , Chang-Ho Ra , Won Jong Yoo , Jong-Hyun Ahn , Jong Hyeok Park, and J. H. C. High-Performance Perovskite Graphene Hybrid Photodetector.Pdf. *Advanced Materials* **2015**, *27*, 41–46.

(25) Do-Hyun Kwak, Da-Hye Lim, Hyun-Soo Ra, P. R. and J.-S. L. High Performance Hybrid Graphene–CsPbBr3Ix.Pdf. *RSC Advances* **2016**, *6*, 65252. https://doi.org/DOI: 10.1039/c6ra08699c.

(26) Chen, J.; Jing, Q.; Xu, F.; Lu, Z.; Lu, Y. High-Sensitivity Optical-Fiber-Compatible Photodetector with an Integrated CsPbBr_3–Graphene Hybrid Structure. *Optica* **2017**, *4* (8), 835. https://doi.org/10.1364/optica.4.000835.

(27) Wang, J.; Da, P.; Zhang, Z.; Luo, S.; Liao, L.; Sun, Z.; Shen, X.; Wu, S.; Zheng, G.; Chen, Z. Lasing from Lead Halide Perovskite Semiconductor

Microcavity System. *Nanoscale* **2018**, *10* (22), 10371–10376. https://doi.org/10.1039/c8nr01350k.

(28) Kang, J.; Li, J.; Wei, S. H. Atomic-Scale Understanding on the Physics and Control of Intrinsic Point Defects in Lead Halide Perovskites. *Applied Physics Reviews* **2021**, *8* (3), 031302. https://doi.org/10.1063/5.0052402.

(29) Ahmed, G. H.; El-Demellawi, J. K.; Yin, J.; Pan, J.; VELUSAMY, D. B.; Hedhili, M. N.; Alarousu, E.; Bakr, O. M.; Alshareef, H. N.; Mohammed, O. F. Giant Photoluminescence Enhancement in CsPbCl3 Perovskite Nanocrystals by Simultaneous Dual-Surface Passivation. *ACS Energy Letters* **2018**, *3*, 2301–2307. https://doi.org/10.1021/acsenergylett.8b01441.

(30) Pan, J.; Li, X.; Gong, X.; Yin, J.; Zhou, D.; Sinatra, L.; Huang, R.; Liu, J.; Chen, J.; Dursun, I.; El-Zohry, A. M.; Saidaminov, M. I.; Sun, H. T.; Mohammed, O. F.; Ye, C.; Sargent, E. H.; Bakr, O. M. Halogen Vacancies Enable Ligand-Assisted Self-Assembly of Perovskite Quantum Dots into Nanowires. *Angewandte Chemie - International Edition* **2019**, *58* (45), 16077–16081. https://doi.org/10.1002/anie.201909109.

(31) Chen, B.; Rudd, P. N.; Yang, S.; Yuan, Y.; Huang, J. Imperfections and Their Passivation in Halide Perovskite Solar Cells. *Chemical Society Reviews* **2019**, *48* (14), 3842–3867. https://doi.org/10.1039/c8cs00853a.

(32) Lei, D. Y.; Li, J.; Ong, H. C. Tunable Surface Plasmon Mediated Emission from Semiconductors by Using Metal Alloys. *Applied Physics Letters* **2007**, *91* (2). https://doi.org/10.1063/1.2752770.

(33) Li, J.; Ong, H. C. Temperature Dependence of Surface Plasmon Mediated Emission from Metal-Capped ZnO Films. *Applied Physics Letters* **2008**, *92* (12), 2006–2009. https://doi.org/10.1063/1.2902323.

(34) Lu, Y. C.; Chen, C. Y.; Yeh, D. M.; Huang, C. F.; Tang, T. Y.; Huang, J. J.; Yang, C. C. Temperature Dependence of the Surface Plasmon Coupling with an InGaNGaN Quantum Well. *Applied Physics Letters* **2007**, *90* (19). https://doi.org/10.1063/1.2738194.

(35) Chen, Y. L.; Ma, Y. J.; Chen, D. D.; Wang, W. Q.; Ding, K.; Wu, Q.; Fan, Y. L.; Yang, X. J.; Zhong, Z. Y.; Xu, F.; Jiang, Z. M. Effect of Graphene on Photoluminescence Properties of Graphene/GeSi Quantum Dot Hybrid Structures. *Applied Physics Letters* **2014**, *105* (2), 021104. https://doi.org/10.1063/1.4889890.

(36) Farhat, M.; Guenneau, S.; Bağci, H. Exciting Graphene Surface Plasmon Polaritons through Light and Sound Interplay. *Physical Review Letters* **2013**, *111* (23), 237404. https://doi.org/10.1103/PhysRevLett.111.237404.

(37) Hwang, S. W.; Shin, D. H.; Kim, C. O.; Hong, S. H.; Kim, M. C.; Kim, J.; Lim, K. Y.; Kim, S.; Choi, S. H.; Ahn, K. J.; Kim, G.; Sim, S. H.; Hong, B. H. Plasmon-Enhanced Ultraviolet Photoluminescence from Hybrid Structures of Graphene/ZnO Films. *Physical Review Letters* **2010**, *105* (12), 127403. https://doi.org/10.1103/PhysRevLett.105.127403.

(38) Chen, Y.; Dong, Z.; Wang, B.; Jiang, Z.; Wang, X. The Photoelectric Response of the Graphene/GeSi QDs Hybrid Structure. *Nanotechnology* **2018**, *29* (50).

https://doi.org/10.1088/1361-6528/aae3c8.

(39) Swarnkar, A.; Chulliyil, R.; Ravi, V. K.; Irfanullah, M.; Chowdhury, A.; Nag, A. Colloidal CsPbBr3Perovskite Nanocrystals: Luminescence beyond Traditional Quantum Dots. *Angewandte Chemie - International Edition* **2015**, *127* (51), 15644–15648. https://doi.org/10.1002/anie.201508276.

(40) Castañeda, J. A.; Nagamine, G.; Yassitepe, E.; Bonato, L. G.; Voznyy, O.; Hoogland, S.; Nogueira, A. F.; Sargent, E. H.; Cruz, C. H. B.; Padilha, L. A. Efficient Biexciton Interaction in Perovskite Quantum Dots under Weak and Strong Confinement. *ACS Nano* **2016**, *10* (9), 8603–8609. https://doi.org/10.1021/acsnano.6b03908.

(41) Krieg, F.; Ochsenbein, S. T.; Yakunin, S.; Ten Brinck, S.; Aellen, P.; Süess, A.; Clerc, B.; Guggisberg, D.; Nazarenko, O.; Shynkarenko, Y.; Kumar, S.; Shih, C. J.; Infante, I.; Kovalenko, M. V. Colloidal CsPbX3(X = Cl, Br, I) Nanocrystals 2.0: Zwitterionic Capping Ligands for Improved Durability and Stability. *ACS Energy Letters* **2018**, *3* (3), 641–646. https://doi.org/10.1021/acsenergylett.8b00035.

(42) Wang, Y.; Li, X.; Song, J.; Xiao, L.; Zeng, H.; Sun, H. All-Inorganic Colloidal Perovskite Quantum Dots: A New Class of Lasing Materials with Favorable Characteristics. *Advanced Materials* **2015**, *27* (44), 7101–7108. https://doi.org/10.1002/adma.201503573.

(43) Song, J.; Li, J.; Li, X.; Xu, L.; Dong, Y.; Zeng, H. Quantum Dot Light-Emitting Diodes Based on Inorganic Perovskite Cesium Lead Halides

(CsPbX3). *Advanced Materials* **2015**, *27* (44), 7162–7167. https://doi.org/10.1002/adma.201502567.

(44) Zhao, W.; Wen, Z.; Xu, Q.; Zhou, Z.; Li, S.; Fang, S.; Chen, T.; Sun, L.; Wang, X.; Liu, Y.; Sun, Y.; Tan, Y. W.; Dai, N.; Hao, J. Remarkable Photoluminescence Enhancement of CsPbBr3 Perovskite Quantum Dots Assisted by Metallic Thin Films. *Nanophotonics* **2021**, *10* (8), 2257–2264. https://doi.org/10.1515/nanoph-2021-0064.

(45) Hendrik Utzat, Weiwei Sun, Alexander E. K. Kaplan, Franziska Krieg, Matthias Ginterseder, Boris Spokoyny, Nathan D. Klein, Katherine E. Shulenberger, Collin F. Perkinson, Maksym V. Kovalenko, M. G. B. Coherent Single-Photon Emission from Colloidal Lead Halide Perovskite Quantum Dots. *Science* **2019**, *363* (March), 1068–1072.

(46) Xiong, Q.; Huang, S.; Du, J.; Tang, X.; Zeng, F.; Liu, Z.; Zhang, Z.; Shi, T.; Yang, J.; Wu, D.; Lin, H.; Luo, Z.; Leng, Y. Surface Ligand Engineering for CsPbBr3 Quantum Dots Aiming at Aggregation Suppression and Amplified Spontaneous Emission Improvement. *Advanced Optical Materials* **2020**, *8* (20), 2000977. https://doi.org/10.1002/adom.202000977.

(47) Ying, G.; Jana, A.; Osokin, V.; Farrow, T.; Taylor, R. A.; Park, Y. Highly Efficient Photoluminescence and Lasing from Hydroxide Coated Fully Inorganic Perovskite Micro/Nano-Rods. *Advanced Optical Materials* **2020**, *8* (23), 2001235. https://doi.org/10.1002/adom.202001235.

(48) Jun Pan, Xiyan Li, Xiwen Gong, Jun Yin, Dianli Zhou, Lutfan Sinatra, Renwu

Huang, Jiakai Liu, Jie Chen, Ibrahim Dursun, Ahmed M. El-Zohry, Makhsud I. Saidaminov, Hong-Tao Sun, Omar F. Mohammed, Changhui Ye, Edward H. Sargent, abd O. M. B. Halogen Vacancies Enable Ligand-Assisted Self-Assembly of Perovskite Quantum Dots into.Pdf. *Angew.Chem. Int.Ed* **2019**, *58*, 16077–16081.

(49) Yin, J.; Yang, H.; Song, K.; El-Zohry, A. M.; Han, Y.; Bakr, O. M.; Brédas, J. L.; Mohammed, O. F. Point Defects and Green Emission in Zero-Dimensional Perovskites. *Journal of Physical Chemistry Letters* **2018**, *9* (18), 5490–5495. https://doi.org/10.1021/acs.jpclett.8b02477.

(50) Joucken, F.; Tison, Y.; Lagoute, J.; Dumont, J.; Cabosart, D.; Zheng, B.; Repain, V.; Chacon, C.; Girard, Y.; Botello-Méndez, A. R.; Rousset, S.; Sporken, R.; Charlier, J. C.; Henrard, L. Localized State and Charge Transfer in Nitrogen-Doped Graphene. *Physical Review B - Condensed Matter and Materials Physics* **2012**, *85* (16), 161408(R). https://doi.org/10.1103/PhysRevB.85.161408.

(51) Li, J.; Cushing, S. K.; Meng, F.; Senty, T. R.; Bristow, A. D.; Wu, N. Plasmon-Induced Resonance Energy Transfer for Solar Energy Conversion. *Nature Photonics* **2015**, *9* (9), 601–607. https://doi.org/10.1038/nphoton.2015.142.

(52) Yao, K.; Li, S.; Liu, Z.; Ying, Y.; Dvořák, P.; Fei, L.; Šikola, T.; Huang, H.; Nordlander, P.; Jen, A. K. Y.; Lei, D. Plasmon-Induced Trap Filling at Grain Boundaries in Perovskite Solar Cells. *Light: Science and Applications* **2021**, *10* (1), 219. https://doi.org/10.1038/s41377-021-00662-y.

(53) Huang, X.; Li, H.; Zhang, C.; Tan, S.; Chen, Z.; Chen, L.; Lu, Z.; Wang, X.; Xiao, M. Efficient Plasmon-Hot Electron Conversion in Ag–CsPbBr3 Hybrid Nanocrystals. *Nature Communications* **2019**, *10* (1), 1163. https://doi.org/10.1038/s41467-019-09112-1.

(54) Koichi Okamoto, Mitsuru Funato, Yoichi Kawakami, K. T. High-Efficiency Light Emission by Means of Exciton–Surface-Plasmon Coupling.Pdf. *Journal of Photochemistry and Photobiology C: Photochemistry Reviews* **2017**, *32*, 58–77.

(55) Liu, Y.; Willis, R. F.; Emtsev, K. V.; Seyller, T. Plasmon Dispersion and Damping in Electrically Isolated Two-Dimensional Charge Sheets. *Physical Review B - Condensed Matter and Materials Physics* **2008**, *78* (20), 201403(R). https://doi.org/10.1103/PhysRevB.78.201403.

(56) Liu, Y.; Willis, R. F. Plasmon-Phonon Strongly Coupled Mode in Epitaxial Graphene. *Physical Review B - Condensed Matter and Materials Physics* **2010**, *81* (8), 081406(R). https://doi.org/10.1103/PhysRevB.81.081406.

(57) Filip, M. R.; Haber, J. B.; Neaton, J. B. Phonon Screening of Excitons in Semiconductors: Halide Perovskites and Beyond. *Physical Review Letters* **2021**, *127* (6), 67401. https://doi.org/10.1103/PhysRevLett.127.067401.

(58) Milena De Giorgi, Mohammad Ramezani, Francesco Todisco, Alexei Halpin, Davide Caputo, Antonio Fieramosca, Jaime Gomez-Rivas, and D. S. Interaction and Coherence of a Plasmon−Exciton Polariton Condensate. *ACS Photonics* **2018**, *5*, 3666–3672. https://doi.org/DOI:

10.1021/acsphotonics.8b00662.

(59) Hofmann, C.; Kuhn, S. Strong Coupling in a Single Quantum Dot–Semiconductor Microcavity System. *Nature* **2004**, *432*, 197–200. https://doi.org/10.1038/nature02969.